

## Interatomic potential, phonon spectrum, and molecular-dynamics simulation up to 1300 K in $\text{YBa}_2\text{Cu}_3\text{O}_{7-\delta}$

S. L. Chaplot

*Nuclear Physics Division, Bhabha Atomic Research Centre, Bombay 400 085, India*

(Received 20 September 1989; revised manuscript received 3 January 1990)

An interatomic potential for  $\text{YBa}_2\text{Cu}_3\text{O}_{7-\delta}$  based on Coulomb and short-range interactions is proposed. The calculated minimum energy structure, phonon spectrum, and the results of the molecular-dynamics computer simulation up to 1300 K on thermal expansion and the orthorhombic-to-tetragonal phase transition are in fair agreement with reported experiments.

### INTRODUCTION

A wealth of experimental data has been accumulated on the ceramic superconductors and related materials that belong to the perovskite<sup>1</sup> family of crystal systems. We draw attention in particular to the detailed crystal structure,<sup>2,3</sup> phase transitions,<sup>3</sup> phonon spectra,<sup>2(b),4</sup> and related macroscopic properties. It would be of considerable value if such a range of data could be understood in terms of an interatomic potential. A potential model can provide much useful additional information about the microscopic properties, e.g., using the molecular-dynamics simulation. We may refer to the recent studies on the empirical interatomic potential for silicon<sup>5</sup> and carbon.<sup>6</sup> Given the complexity of the perovskite superstructures, such as  $\text{YBa}_2\text{Cu}_3\text{O}_{7-\delta}$ , a potential model would have to be empirical at the present stage of development.<sup>7-10</sup> An *ab initio* calculation<sup>11</sup> for  $\text{La}_2\text{CuO}_4$ , although useful and interesting, has only produced numerical results that are in rough qualitative agreement with experiments.

In this paper we propose the first empirical interatomic potential model for  $\text{YBa}_2\text{Cu}_3\text{O}_{7-\delta}$  (Y-Ba-Cu-O), which gives predictions on the structure and dynamics up to 1300 K that are close to the observed values. While other attempts were made in predicting either the structure<sup>9</sup> or dynamics<sup>10</sup> at low temperature, we earlier reported<sup>7</sup> a model that is suitable for both the structure and dynamics for the  $\delta=0$  system at low temperatures, and the model was improved<sup>8</sup> further for use in molecular-dynamics simulation at high temperatures beyond the traditional harmonic approximation restricting to small-amplitude vibrational dynamics. Recent neutron inelastic scattering measurements<sup>4(c)</sup> of a few low-energy branches of the phonon dispersion relation are in good agreement with our earlier prediction<sup>7</sup> for  $\delta=0$ , with only about 10% average discrepancy. Since the Y-Ba-Cu-O systems exist with *different* values of the oxygen contents ( $\delta=0-1$ ), in this paper we propose a model interatomic potential for use with such different oxygen contents and demonstrate its various applications.

### INTERATOMIC POTENTIAL

We consider an unscreened rigid-ion model.<sup>7</sup> A detailed justification for the use of this model for the Y-Ba-

Cu-O class of ceramic compounds at the present stage of development is given in Ref. 7, in particular for ignoring the metallic screening for the  $\delta=0$  case in  $\text{YBa}_2\text{Cu}_3\text{O}_{7-\delta}$ . The simple model gives a very good qualitative account of many of the observed structural and dynamical properties of this important material as shown in this paper. Therefore we believe that the interatomic forces that govern the statics and dynamics of the ceramic superconductors are substantially ionic in nature. A two-body potential function of the following form is used:

$$V_{kk'}(r_{ij}) = \frac{e^2 Z(k)Z(k')}{4\pi\epsilon_0 r_{ij}} + a \exp\left[\frac{-br_{ij}}{R(k)+R(k')}\right] - \frac{w}{r_{ij}^6} - cD \exp\left[\frac{-n(r_{ij}-r_0)^2}{2cr_{ij}}\right]. \quad (1)$$

Here  $e^2/(4\pi\epsilon_0) = 144 \text{ eV/nm}$ ,  $a = 1822 \text{ eV}$ ,  $b = 12.364$ , and  $r_{ij}$  is the distance between the two atoms of species  $k$  and  $k'$ . The choice and significance of the values of  $a$ ,  $b$ , and the adjustable parameters,  $Z(k)$  and  $R(k)$  is discussed in Ref. 7. The third and fourth terms in Eq. (1) are found<sup>8</sup> to be important in determining the structural stability and dynamics at high temperatures. The third term is assumed to act only between the oxygen atoms. The fourth term, a covalent potential of the Lippincott-Schroeder type, is assumed between pairs of copper and oxygen atoms that are either in the  $\text{CuO}_2$  planes or in the  $\text{CuO}_3$  chain networks. Other parameters are chosen<sup>8</sup> as  $w = 50 \times 10^{-6} \text{ eV nm}^6$ ,  $c = 0.5$ ,  $D = 1 \text{ eV}$ ,  $n = 80 \text{ nm}^{-1}$ , and  $r_0 = 0.18 \text{ nm}$ . This potential is used in all the applications reported in this paper.

While the relative values of the charges on different atoms are determined from the requirement of producing a stable and reasonable crystal structure, they have been scaled to ensure the maximum of the phonon frequencies to be approximately of the right magnitude<sup>7</sup>. Table I gives the values of the parameters for the cases of  $\delta=0$  and 1, from which the values corresponding to other  $\delta$  ( $0 < \delta < 1$ ) are interpolated. Charge neutrality condition for the unit cell was imposed as required in the rigid-ion model. Note that, with the loss of one oxygen atom from  $\delta=0$  to 1, we determined from the stability requirements that the positive charge is essentially depleted from the Cu(1) and Ba atoms only, which may be of significance

TABLE I. Interatomic potential parameters for  $\text{YBa}_2\text{Cu}_3\text{O}_{7-\delta}$ . The labeling of atoms is as per Table II.

Atom	Z	$\delta=0$	Z	$\delta=1$
		R (nm)		R (nm)
Y	1.9	0.178	1.9	0.178
Ba	1.5	0.230	1.25	0.210
Cu(1)	1.4	0.120	0.6	0.110
Cu(2)	1.4	0.120	1.4	0.120
O	-1.3	0.174	-1.3	0.174

with respect to the superconductivity of the  $\delta=0$  system. Our oxygen charge of  $-1.3$  is smaller than the value of  $-1.7$  obtained<sup>11(c)</sup> by comparing the self-consistent charge density from a band-structure calculation to an adjustable ionic model. The empirical effective charge in a lattice-dynamical rigid-ion model is usually smaller than the true ionic charge as it effectively compensates for the neglect of polarization of ions during vibrations.

### STRUCTURE AND PHONON SPECTRUM

The minimum-energy structure and the lattice dynamics are calculated using the current version of the program<sup>12</sup> DISPR. Table II gives the calculated equilibrium structure and its comparison with recent neutron diffraction data,<sup>2</sup> which shows fair agreement. The observed relative shifts of various atoms between the  $\delta=0$

TABLE II. The calculated minimum potential structure of  $\text{YBa}_2\text{Cu}_3\text{O}_{7-\delta}$ , compared to the reported (Ref. 2) neutron diffraction results given in parentheses. The experimental (Ref. 2)  $a$ ,  $b$ , and  $c$ , at 300 K have been decreased to correspond to 0 K. The fractional atomic coordinates are Y (0.5,0.5,0.5), Ba (0.5,0.5, $z_1$ ), Cu(1) (0,0,0), Cu(2) (0,0, $z_2$ ), O(1) (0,0, $z_3$ ), O(2) (0.5,0, $z_4$ ), O(3) (0,0.5, $z_5$ ), and O(4) (0,0.5,0).

	$\delta=0$	$\delta=1$
$a$ (nm)	0.380(0.381)	0.376(0.383)
$b$ (nm)	0.382(0.387)	0.376(0.383)
$c$ (nm)	1.169(1.163)	1.175(1.174)
$z_1$	0.189(0.184)	0.204(0.194)
$z_2$	0.352(0.355)	0.350(0.361)
$z_3$	0.162(0.158)	0.160(0.153)
$z_4$	0.380(0.378)	0.380(0.379)
$z_5$	0.380(0.377)	0.380(0.379)

and 1 cases are qualitatively reflected in the calculated structures. The present potential is also used to calculate the pressure dependence of the structure and phonon frequencies. The calculated values of the bulk modulus and its pressure derivative are given in Table III and compared with available data.

The calculated one-phonon density of states is given in Fig. 1. For comparison with the inelastic neutron scattering data, we also give in Fig. 1, the “neutron-weighted” phonon density of states, which involves the

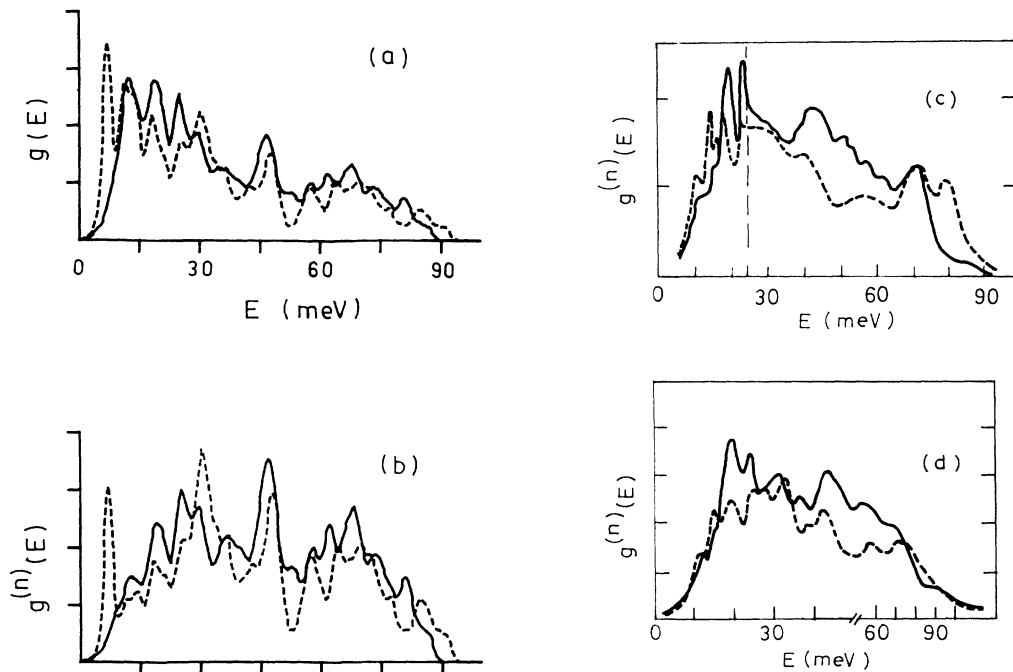


FIG. 1. The calculated phonon spectra: (a) density of states  $g(E)$  and (b) the neutron-weighted density of states  $g^{(n)}(E)$ . The solid and dashed lines are for  $\text{YBa}_2\text{Cu}_3\text{O}_7$  and  $\text{YBa}_2\text{Cu}_3\text{O}_6$ , respectively. Gaussian smoothing with full width at half maximum of 2 meV is included. The experimental spectra corresponding to (b) as obtained from inelastic neutron scattering are given in (c) from Ref. 2(b), and in (d) from Ref. 4(a). The energy resolution in (c) was estimated to be nearly 3 meV and 10 meV for energies below and above 25 meV, respectively. The resolution in (d) gradually changed from 1 to 10 meV for energies from 10 to 90 meV.

TABLE III. Bulk modulus  $B_0$  and its pressure derivative  $B'_0$  for  $\text{YBa}_2\text{Cu}_3\text{O}_{7-\delta}$ .

	Calculated		Experimental		
	$\delta=0$	$\delta=1$	Ref. 13(a)	$\delta \approx 0$ Ref. 13(b)	Ref. 13(c)
$B_0$ (GPa)	109	92	157	95	65
$B'_0$	4.1	5.0	2.9		$\sim 50$

neutron-scattering-weight factors.<sup>7</sup> This factor for the atomic species Y, Ba, Cu, and O is 0.0849, 0.0252, 0.1178, and 0.2647 barns/amu, respectively, the largest being for the oxygens. The calculations are in fair agreement with the various experimental spectra.<sup>2(b),4</sup> In particular, the changes in the spectra in going from  $\delta=0$  to 1 are well reproduced in the calculation with regard to the shift in the low-energy region, lowering of the density in the middle-energy region, and extending of the spectrum in the high-energy region. The strong low-energy peak at 7.5 meV in the calculation in the  $\delta=1$  case is not evident in the experiments but may be compared with the weaker peak at about 10 meV. Figure 2 compares the contribu-

tions of the different atoms and different polarizations to the phonon spectrum. As discussed in detail in Ref. 7 for  $\delta=0$ , the thermal vibrational amplitudes, the calculated lattice contribution to the specific heat, and the Debye temperature are in fair agreement with reported experiments.

### MOLECULAR-DYNAMICS SIMULATION

The high-temperature behavior of the system is obtained by computer simulation based on a constant-pressure molecular-dynamics technique, using a computer program developed by us.<sup>8,14</sup> Of particular interest here is the orthorhombic-to-tetragonal phase transition reported<sup>3</sup> to occur at a temperature  $T_c$  of about 970 K in the oxygen-deficient system  $\text{YBa}_2\text{Cu}_3\text{O}_{7-\delta}$  ( $\delta \approx 0.5$ ). The transition essentially involves the disordering of certain oxygen atoms in the  $ab$  plane in the tetragonal phase from their ordered arrangement along the  $b$  direction in Cu-O chains in the orthorhombic phase. The simulation is intended to illustrate the success of the potential model with regard to this phase transition and to study the accompanying atomic dynamics and average distributions.

Each simulation run is carried out for 9000 time steps of 0.005 psec on a macrocell made of  $2a$ ,  $2b$ , and  $c$  with periodic boundary conditions. This macrocell is considered sufficient for the purpose of the chain disordering transition, and it is found suitable for efficiently performing a large number of different simulations with different oxygen contents and for various temperatures up to 1300 K. For the cases of  $\delta=0$ , 0.25, and 0.5, the orthorhombic-to-tetragonal transition is observed at 1100, 1000, and 900 K, respectively, when the O(4) (0,0.5,0) and O(5) (0.5,0,0) sites become nearly equally populated. It is known from experiments<sup>3</sup> that the system loses oxygen when heated under ambient atmospheric pressure. We believe that the oxygen loss occurs through the surface of the real system, which is not included in the present simulation. However, we note with satisfaction, that the present result on the tetragonal transition temperature of about 1000 K is in good agreement with experimental results.<sup>3</sup>

In addition, the zero-pressure simulation as a function of temperature reproduces the experimental average volume thermal expansion<sup>3</sup> of  $6 \times 10^{-5} \text{ K}^{-1}$  between 0 K and  $T_c$ . We also observe large diffusion of all atoms above 1300 K, which is close to the experimental melting temperature.<sup>15</sup>

The simulation gives the details of the oxygen jump dynamics at high temperatures, both in terms of the jump paths in real space and the time scale of the jumps. As an illustration, we show in Fig. 3 the XY and YZ projections

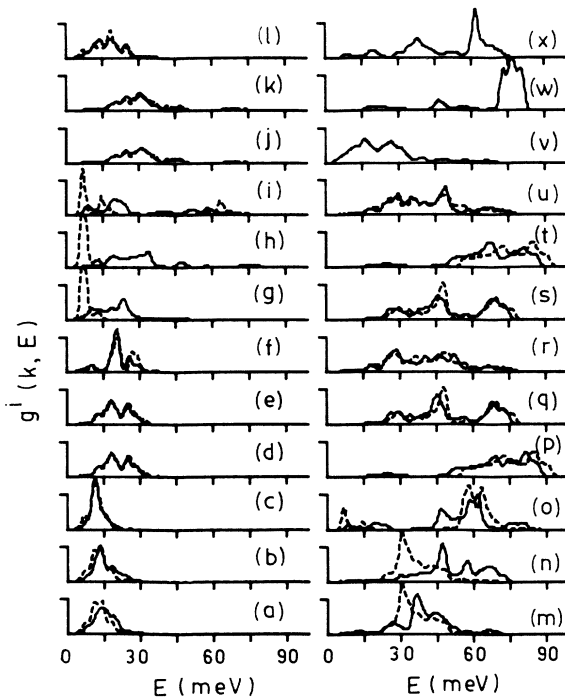


FIG. 2. The calculated partial components  $g^i(k, E)$  of the phonon density of states corresponding to the different atoms  $k$  and polarization along the different directions  $i$ . The  $k$  and  $i$  for the different curves are as follows: (a) Ba,  $x$ ; (b) Ba,  $y$ ; (c) Ba,  $z$ ; (d) Y,  $x$ ; (e) Y,  $y$ ; (f) Y,  $z$ ; (g) Cu(1),  $x$ ; (h) Cu(1),  $y$ ; (i) Cu(1),  $z$ ; (j) Cu(2),  $x$ ; (k) Cu(2),  $y$ ; (l) Cu(2),  $z$ ; (m) O(1),  $x$ ; (n) O(1),  $y$ ; (o) O(1),  $z$ ; (p) O(2),  $x$ ; (q) O(2),  $y$ ; (r) O(2),  $z$ ; (s) O(3),  $x$ ; (t) O(3),  $y$ ; (u) O(3),  $z$ ; (v) O(4),  $x$ ; (w) O(4),  $y$ ; (x) O(4),  $z$ . The spectra from (a) to (l) have been normalized to 1, and those from (m) to (x) to 2. The solid and dashed lines are for  $\text{YBa}_2\text{Cu}_3\text{O}_7$  and  $\text{YBa}_2\text{Cu}_3\text{O}_6$  respectively. Gaussian smoothing with full width at half maximum of 2 meV is included.

of the oxygen motions in the  $\text{CuO}_3$  network for a period of 10 psec at 1000 K, close to the chain disordering transition for  $\delta=0.25$ . In this figure one can see the projection of the thermal vibrations of the oxygen atoms about their equilibrium sites and also the jump motions between temporary equilibrium sites. As shown in Fig. 4, during

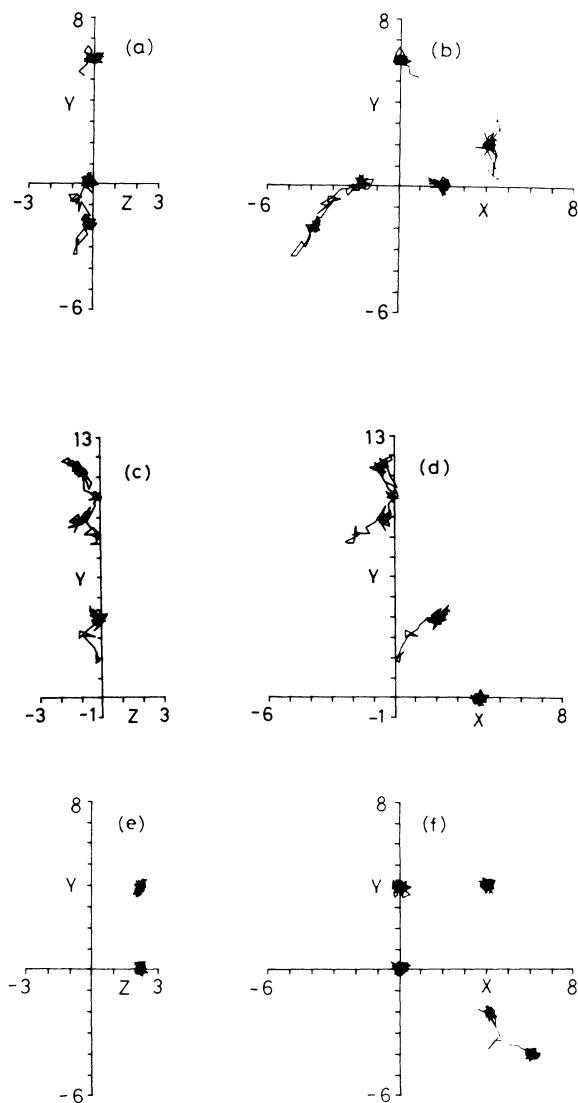


FIG. 3. Observation of oxygen jumps and distribution as observed in the molecular dynamics simulation of  $\text{YBa}_2\text{Cu}_3\text{O}_{6.75}$  at 1000 K. The  $XY$  and  $YZ$  projections of the atomic coordinates for a duration of 10 psec are given. Angstrom ( $=0.1$  nm) units are used. Separate projections are given for the oxygen atoms, which were in different layers along the  $Z$  axis at the start of the simulation ( $t=0$ , as in the orthorhombic phase). The projections correspond to the time  $t=35-45$  psec. The  $YZ$  projections are shown only of the two atoms in each layer, which at the start at  $t=0$  have  $0 \leq X < a$ . The  $XY$  projections include all the atoms in each layer. (a)  $YZ$  and (b)  $XY$  projections of the atoms starting at the O(1) sites at  $Z=-0.16c$ . (c)  $YZ$  and (d)  $XY$  projections of the atoms starting at the O(4) sites at  $Z=0$ . (e)  $YZ$  and (f)  $XY$  projections of the atoms starting at the O(1) sites at  $Z=0.16c$ .

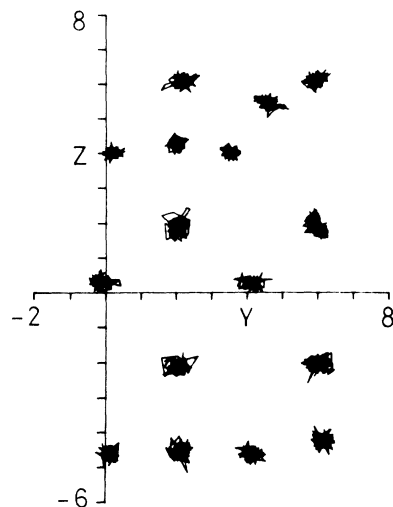


FIG. 4. The thermal motions of the cations and the O(3) atoms, as observed in the molecular-dynamics simulation of  $\text{YBa}_2\text{Cu}_3\text{O}_{6.75}$  at 1000 K. The  $YZ$  projections of the atomic coordinates for a duration of 10 psec are given. Angstrom ( $=0.1$  nm) units are used. From the  $2a \times 2b \times c$  macrocell only the  $0 \leq X < a$  part is projected. The O(2) atoms are not projected, since they fall close to the Cu(2) atoms, but their behavior is similar to that of the O(3) atoms.

the same period of 10 psec the heavy atoms and the oxygens in the  $\text{CuO}_2$  planes showed essentially small amplitude vibrations about their respective average positions. We note, however, that for the duration of any jump motion, the other atoms in the neighborhood of the jumping atom also relax from their otherwise undisturbed positions.

At the transition the oxygen atoms in the  $\text{CuO}_3$  network undergo frequent jump motions, at the rate of about 10 jumps per nsec per oxygen atom. We observe that vacancies are also created at  $T_c$  at the oxygen atom site O(1), which links the atoms Cu(1) and Cu(2). Such vacant sites are about 10% in the  $\delta=0$  case and increase up to 25% in the  $\delta=0.5$  case, which is in qualitative agreement with suggestions from experiments.<sup>3(b),16</sup> At  $T_c + 100$  K, jumps are also observed among the O(2), O(3) and O(6) (0,0,0.5) sites with about 20% vacancies in the  $\text{CuO}_2$  plane, giving almost equal distribution at all these sites. The oxygen jump dynamics may be investigated by neutron quasielastic scattering as used<sup>17</sup> to study the fluorine motions in the superionic conductor  $\text{CaF}_2$ . We expect quasielastic widths of the order of  $10 \mu\text{eV}$  at momentum transfer of about  $2 \text{ \AA}^{-1}$ . The oxygen diffusion in Y-Ba-Cu-O has also been studied qualitatively by perturbed angular correlation spectroscopy.<sup>18</sup> We may expect the jumps paths to be slightly sensitive to the presence of weak three-body interactions.

We have also carried out the molecular dynamics simulation at low temperatures to supplement, as well as to look for, possible deviations from the results of lattice statics calculation. The latter study involves the potential energy minimization and assumes the space-group symmetry, that is, the special atomic positions and the

periodicity of the unit cell. The molecular dynamics study, on the other hand, allows free movement of atoms, and periodicity is only assumed over the bigger macrocell. In simulation at low temperature, below 300 K, for  $\delta=0$  and 0.25, we observe the chain oxygen O(4) shifted perpendicular to the chain by about 0.5 Å, which is also a possibility suggested from recent neutron diffraction experiments.<sup>2(c)</sup> For the  $\delta \geq 0.50$  case we observe the O(4) atoms shifted to the (0.5,0.5,0) sites at low temperature, which might be expected from a two-body potential model. Simulation at high temperatures, however, shows lowering of the occupancy at the (0.5,0.5,0) site and increase at the (0,0.5,0) site.

A possible connection between highly anharmonic vibrations and superconductivity has been suggested.<sup>19</sup> The vibration of the chain oxygen O(4) perpendicular to the chain is particularly soft<sup>7</sup> and anharmonic. We obtain the same qualitative behavior by using slightly different values of the potential parameters which nearly reproduce the observed structure.

### CONCLUSION

In conclusion, we have made an attempt to develop a model interatomic potential for  $\text{YBa}_2\text{Cu}_3\text{O}_{7-\delta}$ , which is aimed at being consistent with the structure, dynamics, and related properties from low temperature up to melting and also at high pressures. It is the first time to our knowledge that such a broad spectrum of observed features has been covered using a single model. It has not been possible to cite and make comparison with the large amount of rapidly growing data on Y-Ba-Cu-O systems; instead only a representative is used. The order of

disagreement between the various calculated and observed quantities is found to be only about 10%, which is quite satisfactory for a material of this complexity. This work has thus helped in understanding the important forces at work in determining the structure and dynamics of the ceramic superconducting materials. Moreover, this simple model predicts the strong anharmonic behavior of certain atomic motions that could be linked<sup>19</sup> to superconductivity.

We have used a simple potential function, since (i) the structure is rather complex and (ii) the potential has to be used in an extensive molecular-dynamics computer simulation to study the high-temperature behavior and the order-disorder phase transition. Thus we have omitted the inclusion of the electronic polarizability as in a shell model,<sup>10</sup> the screening<sup>20</sup> due to the small density of conduction electrons in the  $\delta=0$  case, and many-body terms in the potential. The effects of these omissions are expected to be small for the general applications we have considered, though their inclusion would improve the numerical accuracy. Further improvement of the model potential may be made when sufficient experimental data become available on the structure and detailed phonon dispersion relation, and their pressure and temperature dependence. The present model potential is also suitable for other applications such as the study of structure and dynamics of defects and surfaces.

### ACKNOWLEDGMENTS

The author appreciates the encouragement given by Dr. K. R. Rao and Dr. B. A. Dasannacharya.

<sup>1</sup>R. M. Hazen, *Sci. Am.* **258**, 74 (1988).

<sup>2</sup>(a) Earlier references on structure are given in S. L. Chaplot, *Phys. Rev. B* **37**, 7435 (1988); A. Williams, G. H. Kwei, R. B. Von Dreele, A. C. Larson, I. D. Raistrick, and D. L. Bish, *ibid.* **37**, 7960 (1988); (b) B. Renker, F. Gompf, E. Gering, G. Roth, W. Reichardt, D. Ewert, H. Rietschel, and H. Mutka, *Z. Phys. B* **71**, 437 (1988), and references therein; (c) B. Rupp, P. Fischer, E. Pörschke, R. R. Arons, and P. Meuffels, *Physica C* **156**, 559 (1988).

<sup>3</sup>(a) J. D. Jorgensen, M. A. Beno, D. G. Hinks, L. Soderholm, K. J. Volin, R. L. Hitterman, J. D. Grace, I. K. Schuller, C. V. Segre, K. Zhang, and M. S. Kleefisch, *Phys. Rev. B* **36**, 3608 (1987); (b) J. D. Jorgensen, B. W. Veal, W. K. Kwok, G. W. Crabtree, A. Umezawa, L. J. Nowicki, and A. P. Paulikas, *ibid.* **36**, 5731 (1987); (c) A. Ono, *Jpn. J. Appl. Phys.* **26**, L1223 (1987).

<sup>4</sup>(a) I. Natkaniec, A. V. Belushkin, J. Mayer, R. K. Nikolaev, V. K. Fedotov, E. A. Goremychkin, E. G. Ponyatovski, I. L. Sashin, and N. S. Sidorov (unpublished); (b) P. Parshin, M. Zemlyanov, N. Chernoplekov, I. Graboy, and A. Kaul, in *Superconductivity*, edited by V. Ozogin (KIAE, Moscow, 1988), No. 2, p. 30; (c) W. Reichardt, L. Pintschovius, B. Hennion, and F. Collin, *Supercond. Sci. Technol.* **1**, 173 (1988).

<sup>5</sup>E. R. Cowley, *Phys. Rev. Lett.* **60**, 2379 (1988).

<sup>6</sup>J. Tersoff, *Phys. Rev. Lett.* **61**, 2879 (1988).

<sup>7</sup>S. L. Chaplot, *Phys. Rev. B* **37**, 7435 (1988).

<sup>8</sup>S. L. Chaplot, *Phase Transitions* **19**, 49 (1989).

<sup>9</sup>M. Evain, M-H. Whangbo, M. A. Beno, and J. M. Williams, *J. Am. Chem. Soc.* **110**, 614 (1988); R. C. Baetzold, *Phys. Rev. B* **38**, 11 304 (1988).

<sup>10</sup>W. Kress, U. Schröder, J. Prade, A. D. Kulkarni, and F. W. de Wette, *Phys. Rev. B* **38**, 2906 (1988).

<sup>11</sup>(a) R. E. Cohen, W. E. Pickett, L. L. Boyer, and H. Krakauer, *Phys. Rev. Lett.* **60**, 817 (1988); (b) R. E. Cohen, W. E. Pickett, H. Krakauer, and L. L. Boyer, *Physica B* **150**, 61 (1988); (c) H. Krakauer *et al.*, *J. Supercond.* **1**, 111 (1988).

<sup>12</sup>S. L. Chaplot, Bhabha Atomic Research Centre External Report No. BARC-972, 1978 (unpublished).

<sup>13</sup>(a) J. S. Olsen, S. Steenstrup, I. Johannsen, and L. Gerward, *Z. Phys. B* **72**, 165 (1988); see also V. Glaskov, I. Goncharenko, and V. Somenkov, in *Superconductivity*, Ref. 4(b), No. 2, pp. 17; (b) N. V. Jaya, S. Natarajan, S. Natarajan, and G. V. S. Rao, *Solid State Commun.* **67**, 51 (1988); (c) M. Cankurtaran, G. A. Saunders, J. R. Willis, A. Al-Kheffaji, and D. P. Almond, *Phys. Rev. B* **39**, 2872 (1989).

<sup>14</sup>S. L. Chaplot, *Current Sci.* **55**, 949 (1986).

<sup>15</sup>N. V. Chandra Shekar, J. Suresh, K. Govinda Rajan, and G. V. N. Rao, *Bull. Mater. Sci.* **11**, 277 (1988).

<sup>16</sup>K. F. McCarty, J. C. Hamilton, R. N. Shelton, and D. S. Gingley, *Phys. Rev. B* **38**, 2914 (1988).

<sup>17</sup>M. J. Gilan, *J. Phys. C* **19**, 3391 (1986), and references therein.

<sup>18</sup>J. A. Gardner, H. T. Su, A. G. McKale, S. S. Kao, L. L. Peng,

W. H. Warnes, J. A. Sommers, K. Athreya, H. Franzen, and S.-J. Kim, *Phys. Rev. B* **38**, 11 317 (1988); P. Singh, M. N. Nyayate, S. H. Devare, and H. G. Devare, *ibid.* **39**, 2308 (1989).

<sup>19</sup>N. M. Plakida, V. L. Aksenov, and S. L. Drechsler, *Europhys. Lett.* **4**, 1309 (1987); J. R. Hardy and J. W. Flocken, *Phys. Rev. Lett.* **60**, 2191 (1988).

<sup>20</sup>W. Weber and L. F. Mattheiss, *Phys. Rev. B* **37**, 599 (1988).